

Performance optimization of self-powered visible photodetectors based on Cu_2O/electrolyte heterojunctions

Zhi-Ming Bai(白智明), Ying-Hua Zhang(张英华), Zhi-An Huang(黄志安), Yu-Kun Gao(高玉坤), and Jia Liu(刘佳)
Citation: Chin. Phys. B, 2020, 29 (**12**): 128202. DOI: 10.1088/1674-1056/abab7b
Journal homepage: http://cpb.iphy.ac.cn; http://iopscience.iop.org/cpb

What follows is a list of articles you may be interested in

Total dose test with *γ*-ray for silicon single photon avalanche diodes

Qiaoli Liu(刘巧莉), Haiyan Zhang(张海燕), Lingxiang Hao(郝凌翔), Anqi Hu(胡安琪), Guang Wu(吴光), Xia Guo(郭霞)
Chin. Phys. B, 2020, 29 (**8**): 088501. DOI: 10.1088/1674-1056/ab9286

InGaZnO channels

Mei-Na Zhang(张美娜), Yan Shao(邵龑), Xiao-Lin Wang(王晓琳), Xiaohan Wu(吴小晗), Wen-Jun Liu(刘文军), Shi-Jin Ding(丁士进)
Chin. Phys. B, 2020, 29 (**7**): 078503. DOI: 10.1088/1674-1056/ab9738

High-performance midwavelength infrared detectors based on InAsSb nBn design

Xuan Zhang(张璇), Qing-Xuan Jia(贾庆轩), Ju Sun(孙矩), Dong-Wei Jiang(蒋洞微), Guo-Wei Wang(王国伟), Ying-Qiang Xu(徐应强), Zhi-Chuan Niu(牛智川)
Chin. Phys. B, 2020, 29 (**6**): 068501. DOI: 10.1088/1674-1056/ab8377

Highly sensitive polymer photodetectors with a wide spectral response range

Mile Gao(高米勒), Wenbin Wang(王文斌), Lingliang Li(李凌亮), Jianli Miao(苗建利), Fujun Zhang(张福俊)
Chin. Phys. B, 2017, 26 (**1**): 018201. DOI: 10.1088/1674-1056/26/1/018201

In-situ characterization of electrochromism based on ITO/PEDOT:PSS towards preparation of high performance device

Xue-Jin Wang(王学进), Zheng-Fei Guo(郭正飞), Jing-Yu Qu(曲婧毓),Kun Pan(潘坤), Zheng Qi(祁铮), Hong Li(李泓)
Chin. Phys. B, 2016, 25 (**2**): 028201. DOI: 10.1088/1674-1056/25/2/028201

Performance optimization of self-powered visible photodetectors based on Cu_2O/electrolyte heterojunctions*

Zhi-Ming Bai(白智明)†, Ying-Hua Zhang(张英华)‡, Zhi-An Huang(黄志安), Yu-Kun Gao(高玉坤), and Jia Liu(刘佳)

School of Civil and Resource Engineering, University of Science and Technology Beijing, Beijing 100083, *China*

(Received 14 May 2020; revised manuscript received 2 July 2020; accepted manuscript online 1 August 2020)

The performance of the self-powered photodetectors based on the Cu_2O/electrolyte heterojunctions is optimized by adjusting morphology and structure of the Cu_2O film. The Cu_2O film with a deposition time of 2000 s possesses a largest current density of 559.6 μA/cm^2 under visible light illumination at zero bias, with a rising time of 5.2 ms and a recovering time of 9.0 ms. This optimized Cu_2O film has a highest responsivity of about 25.8 mA/W for visible light, and a negligible responsivity for UV light. The high crystallinity and excellent charge transfer property are responsible for the improved photodetection performance.

Keywords: self-powered, visible, photodetector, Cu_2O, photoelectrochemical

PACS: 82.47.Jk, 85.60.Gz, 81.20.Ka, 72.40.+w **DOI:** 10.1088/1674-1056/abab7b

1. Introduction

Self-powered nanodevices with small size and low power consumption are highly desired in areas such as flexible biosensors, smart electronic products, and mobile environmental monitors.[1–3] The self-powered photodetectors can covert a light signal into an electric signal based on photovoltaic effect.[4] Compared with the traditional photoconductive photodetectors, the self-powered photodetectors can operate at zero bias without using batteries or other external power supplies, which makes them more portable and mobile.[5] In addition, they usually have a faster response speed, because the separation process of photogenerated electron–hole pairs in the space charge region is much quicker than the oxygen absorption–desorption process at the nanomaterial surface.[6] Recently, different kinds of self-powered photodetectors, such as p–n junction type,[7–11] Schottky type,[12–14] and photoelectrochemial (PEC) type,[15–17] have drawn much attention. Among them, the PEC-type self-powered photodetector has the advantages of large photoresponsivity, facile fabrication, and abundant raw materials.[18]

The PEC junction at the semiconductor/electrolyte interface has a similar energy band structure to the Schottky junction, which works as a driving force to separate photoinduced carriers and creates a photocurrent without any external power source.[19] Wide band gap metal–oxide-semiconductors, such as ZnO,[20] TiO_2,[21,22] and SnO_2,[23,24] are considered as suitable photoanode materials for the PEC-type self-powered UV photodetectors due to proper energy levels and excellent photoconductive characteristics. The Cu_2O with a narrow band gap (1.9 eV–2.2 eV for the bulk Cu_2O[25]) has been widely used as a visible light absorber in the fields of photovoltaic cells and solar water splitting.[26,27] As an intrinsic p-type semiconductor, it has a large hole mobility of 50 cm^2·V^{-1}·s^{-1}–100 cm^2·V^{-1}·s^{-1} and a high absorbance ranging from blue to green light,[28] making it suitable for the applications in visible detection. In our previous work, the Cu_2O nanomaterials were used to modify the ZnO nanowire arrays to enhance their visible light response.[29,30] Because of low production cost, low preparation temperature, high purity for the products, and controllable stoichiometry and structure, electrochemical deposition method is widely used in metal–oxide synthesis.[31] It has been reported that the morphology, structure, and electrochemical performance can be modified by changing the deposition parameters, such as deposition potential.[32] To the best of our knowledge, the relationship between the deposition parameters and the PEC detection performance is rarely studied. Therefore, the purpose of this work is to investigate the effect of deposition time on the crystal quality and self-powered photodetection properties of the Cu_2O films.

In this work, the Cu_2O films are synthesized via an electrochemical process for the applications in self-powered photodetectors. The morphology, structure, and light absorption properties of the Cu_2O films are regulated by varying the deposition time. The Cu_2O photocathode with a deposition time of 2000 s has the optimized photodetection performance due to larger thickness and better crystal quality. The electrochemical impedance (EIS) results indicate that this photocathode has better charge transfer properties, which contribute to the enhanced performance.

*Project supported by the National Natural Science Foundation of China (Grant No. 51602021) and the Fundamental Research Funds for the Central Universities, China (Grant No. FRF-TP-18-023A2).

†Corresponding author. E-mail: baizhiming2008@126.com

‡Corresponding author. E-mail: zhangyinghuaustb@sina.com

© 2020 Chinese Physical Society and IOP Publishing Ltd

2. Experiment

2.1. Preparation of Cu_2O photoelectrodes

The Cu_2O films were synthesized on the FTO substrates by an electrochemical deposition method.[33] The precursor solution contains 0.2-M $CuSO_4$, 3-M lactic acid, and 77-mL deionized water. The pH value of the solution was adjusted to 12 by adding 4-M NaOH aqueous solution dropwise. A three-electrode system (including an FTO substrate acting as the working electrode with an active area of 0.38 cm^2, an Ag/AgCl reference electrode, and a Pt wire acting as the counter electrode) was used to deposit the Cu_2O films. The precursor solution was kept at 40 °C, and the deposition current was maintained at −0.25 mA by using an electrochemical workstation (CHI660E, CH Instruments Inc.). Corresponding to the deposition times (1000 s, 1500 s, 2000 s, and 3000 s), the samples were denoted as 1.0 K, 1.5 K, 2.0 K, and 3.0 K. Since the volume of the precursor solution is about 200 mL, and the deposition temperature is low, water evaporation during the electrodeposition can be ignored.

2.2. Characterizations

A field emission scanning electron microscope (FE-SEM, FEI QUANTA3D) was used to analyze the morphology. The XRD patterns were measured by using an x-ray diffractometer (Rigaku DMAX-RB using Cu-$K\alpha$ x-ray radiation source). The light absorption and transmission spectra were measured by an ultraviolet-visible-near infrared spectrophotometer (Varian Cary 5000).

The photodetection performance of the self-powered photodetectors were analyzed by a two-electrode system consisting of a Cu_2O working electrode and a Pt counter electrode. The 0.1-M $K_3[Fe(CN)_6]$, $K_4[Fe(CN)_6]$, and KCl aqueous solution (mole ratio 1:1:1) was used as electrolyte. A 300-W xenon lamp (PL S-SXE300, Perfect-Light Co.) with a 0.22-M $NaNO_2$ aqueous solution serving as a filter ($>$ 400 nm) was employed as a visible light source. The EIS plots were measured under a sinusoidal perturbation of 5 mV and a frequency ranging from 100 kHz to 1 Hz. The LEDs (375 nm and 1.1 mW/cm^2; 395 nm and 1.9 mW/cm^2; 470 nm and 8.6 mW/cm^2; 525 nm and 1.6 mW/cm^2; 565 nm and 0.2 mW/cm^2; 590 nm and 1.7 mW/cm^2; 660 nm and 2.4 mW/cm^2) equipped with a DC power supply (BK Precision 1672) were used as a light source to provide monochromatic light for the spectral photoresponse measurement. The photocurrents of the samples at zero bias were measured by using an electrochemical workstation (CHI660E, CH Instruments Inc.).

3. Results and discussion

Figure 1 is the FE-SEM images, showing the morphologies of the Cu_2O films prepared at different deposition time (see Figs. 1(a)–1(h)) and the corresponding size distribution histograms calculated from the FE-SEM images by using a statistical software (see Figs. 1(i) and 1(j)). It can be seen that all the samples are composed of Cu_2O cubes with a preferred growth orientation perpendicular to the FTO substrates. Since some parts of the Cu_2O cubes are covered by others, they look like pyramids. The cubic shape means that the active {100} Cu_2O faces can be exposed to the electrolyte, which is beneficial to the charge transfer at the solid/liquid interface.[27,34] The average side lengths of the cubic Cu_2O particles are 481 ± 79 nm, 581 ± 138 nm, 802 ± 168 nm, and

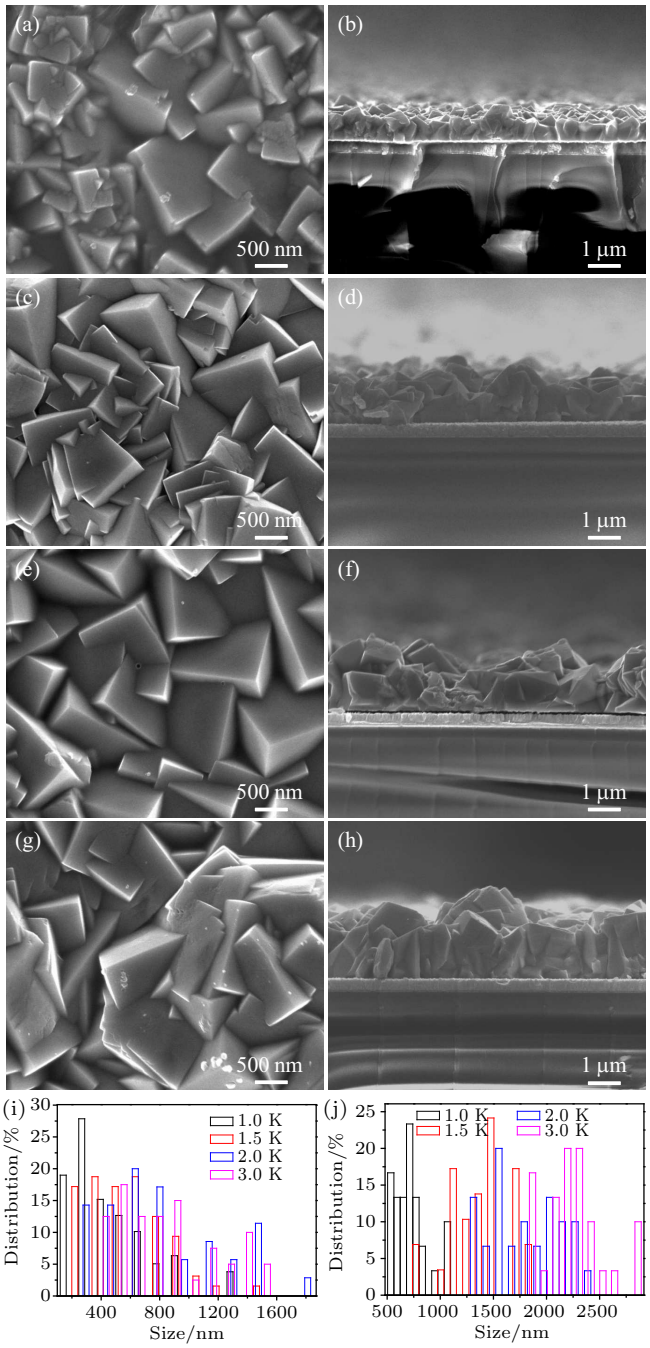


Fig. 1. Top-view and cross-sectional FE-SEM images of [(a), (b)] 1.0-K, [(c), (d)] 1.5-K, [(e), (f)] 2.0-K, and [(g), (h)] 3.0-K samples. Cu_2O particle size distribution histograms calculated from (i) top-view images and (j) cross-sectional FE-SEM images.

829±122 nm for 1.0-K, 1.5-K, 2.0-K, and 3.0-K samples, respectively, and the corresponding thickness values of the Cu_2O films are 719±61 nm, 1359±82 nm, 1792±113 nm, and 2253±145 nm, respectively. For the 2.0-K sample, the individual Cu_2O grains are very smooth and clear outline (Fig. 1(e)). For the 3.0-K sample, although the particle size increases with the growth duration increasing, the surfaces become somewhat deformed (Fig. 1(g)).

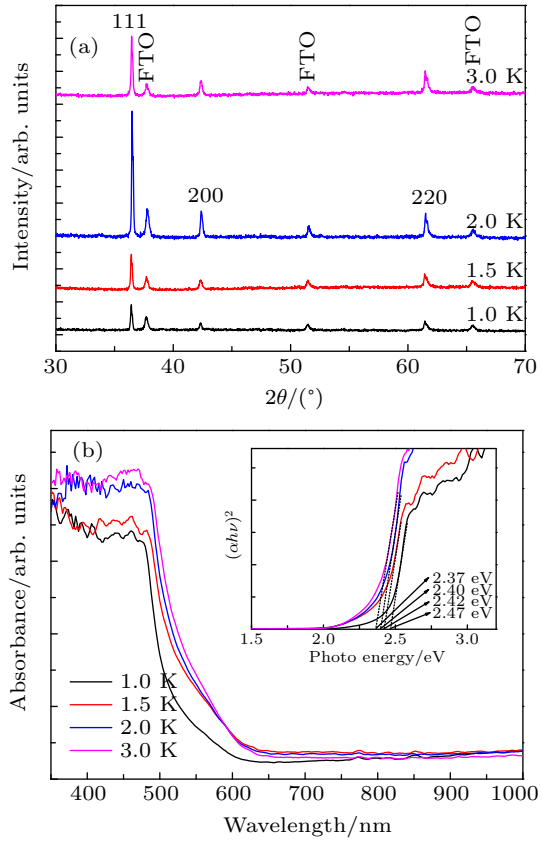


Fig. 2. (a) XRD patterns and (b) UV-Vis absorption spectra of 1.0-K, 1.5-K, 2.0-K, and 3.0-K samples, with insert in panel (b) showing Tauc's plot of respective samples.

In order to further study the effects of the deposition time on the crystal structure of the Cu_2O films, their XRD patterns were measured. It can be seen from Fig. 2(a) that all the samples have strong diffraction peaks at 36.5° corresponding to the (111) plane of Cu_2O, which is consistent with the cubic morphology of the Cu_2O particles. The peaks appearing at 42.4° and 61.7° can be indexed to (200) and (220) planes of cubic Cu_2O (JCPDS 78-2076).[35] The other peaks are generated by the FTO substrate. The intensities of diffraction peaks of Cu_2O become higher with deposition time increasing, which results from the increase of the particle size. However, the diffraction peaks of the 3.0-K sample are lower than those of the 2.0-K sample. In the beginning, the Cu_2O has a preferred growth orientation of {100} and tends to form a tetrahedron in shape. With the increase of deposition time, lactic acid is more easily adsorbed on the polar {100} surfaces, which reduces the surface energy and impedes the growth of Cu_2O perpendicular to {100} facts.[36] Then, the crystal growth rate along the {111} direction gradually increases.[37] The Cu_2O crystal growth along the {111} direction on the {100} plane of the tetrahedron results in the deformation of the surfaces of 3.0 K as shown in Fig. 1(g).

Figure 2(b) shows the UV-vis absorption spectra of the Cu_2O films with different deposition times. All the samples have obvious light absorption in the range between 350 nm and 650 nm, and the light harvesting capacity increases from 1.0-K sample to 3.0-K sample with the increase of the Cu_2O film thickness. The calculated band gap of 1.0-K, 1.5-K, 2.0-K, and 3.0-K samples are 2.47 eV, 2.42 eV, 2.40 eV, and 2.37 eV, respectively (see the inset in Fig. 2(b)). The band gap is observed to be a function of film thickness, which can be due to the Cu–Cu internet work interaction increasing.[38,39] Compared with

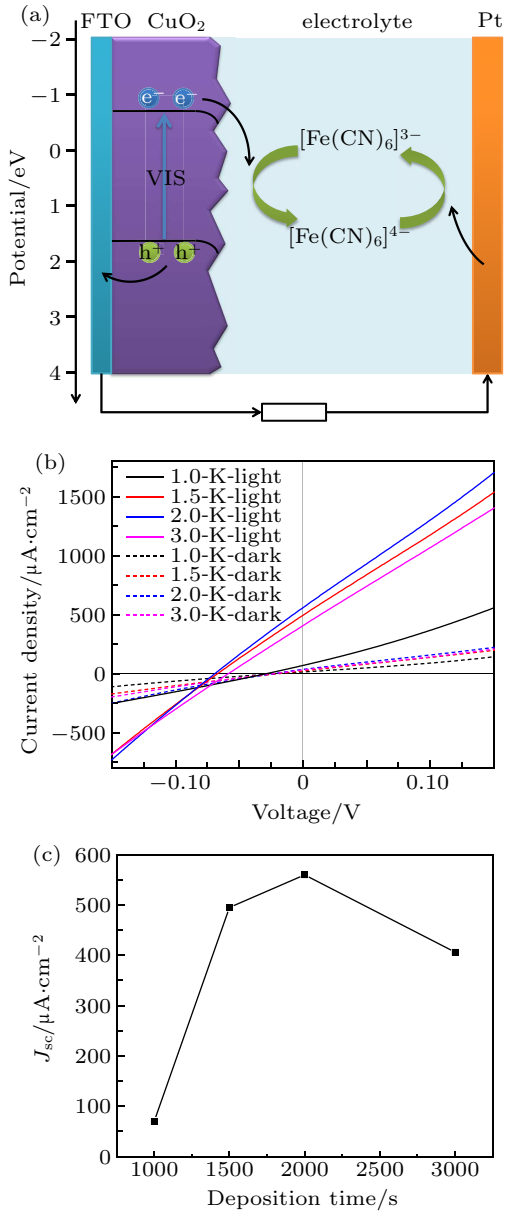


Fig. 3. (a) Energy band diagram of self-powered visible photodetector based on Cu_2O/electrolyte heterojunction. (b) Current density–voltage curves of 1.0-K, 1.5-K, 2.0-K, and 3.0-K samples in the dark and under visible light illumination (> 400 nm, 35 mW/cm^2). (c) Short-circuit current density *versus* deposition time.

the reported band gap of bulk Cu_2O material (2.20 eV), the large band gaps may be correlated with the macro-appearance and structure of the prepared Cu_2O films, which is consistent with the literature data.[28]

Figure 3(a) shows schematically the energy band diagram and working principle of the self-powered photodetector based on the Cu_2O/electrolyte heterojunction. The device has a similar configuration to a dye-sensitized solar cell. When visible light irradiates the Cu_2O film, the photons with energy higher than its band gap excite a lot of electron–hole pairs. The photogenerated charge carriers can be separated by the built-in electric field at the solid/liquid interface. The separated electrons in the conduction band of Cu_2O migrate to the electrolyte and reduce $[Fe(CN)_6]^{3-}$ to $[Fe(CN)_6]^{4-}$.[40] At the same time, the photogenerated holes move from the valance band of Cu_2O to the Pt counter electrode through the external circuit, and capture the electrons from $[Fe(CN)_6]^{4-}$. In this circuit cycle, the space electric field across the Cu_2O/electrolyte interface acts as an 'engine' to drive the transport of the photogenerated charge carriers. Therefore, this photodetector can be directly powered by the incident light signals and operate at zero bias.

To investigate the photodetection performance of the devices, the curve of current density *versus* voltage (J–V) are measured in the dark and under visible light illumination by using a two-electrode system (Fig. 3(b)). All the devices have distinct photoresponse to the visible light (> 400 nm, 35 mW/cm^2) at 0 V, implying that they can operate in photovoltaic mode. As the deposition time increases, the values of short-circuit current density (J_{sc}) increase from 69.9 μA/cm^2 (1.0-K sample), 494.9 μA/cm^2 (1.5-K sample) to 559.6 μA/cm^2 (2.0-K sample). The enhancement in the photocurrent is because the thicker Cu_2O films absorb more incident photons and generate more electron–hole pairs. In addition, the high crystallinity of 2.0 K is beneficial to the charge transport in the Cu_2O film. The open-circuit voltage of 1.0-K, 1.5-K, 2.0-K, and 3.0-K samples are −0.028 V, −0.067 V, −0.069 V, and −0.058 V, respectively. It can be seen from Fig. 3(c) that when the deposition time is 3000 s, the J_{sc} decreases to 406.1 μA/cm^2.

The current–time curves of the self-powered photodetectors under chopped irradiation of the visible light at zero bias are shown in Fig. 4(a). The photocurrent can switch reproducibly between 'on' state and 'off' state. The magnified rising and recovering edges (Figs. 4(b) and 4(c)) of the current response for the 2.0-K sample show that the rising time (time for current to rise from 0 to $1-1/e$) is 5.2 ms, and the recovering time (time for current to recover from 1 to $1/e$) is 9.0 ms.

The spectral responses are measured at zero bias to analyze the selectivity for light of different wavelengths. All the Cu_2O photocathodes have high responses to the visible light (ranging from 470 nm to 660 nm), but low responses to the UV light, because the UV light cannot pass through the electrolyte as shown in Fig. 5(a). Of all samples, the 2.0-K sample has the highest responsivity of 25.8 mA/W at 525 nm, which is about 12.6, 1.1, and 1.4 times the responsivity of 1.0-K, 1.5-K,

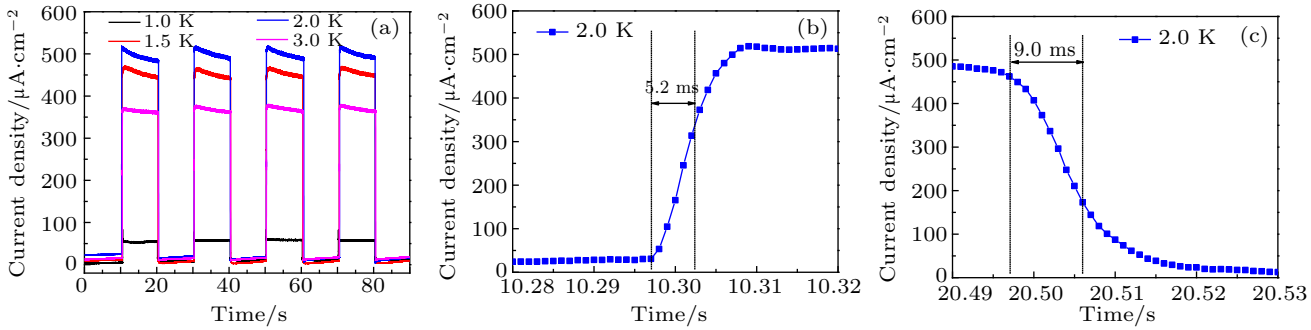


Fig. 4. (a) Time-dependent transient current densities of self-powered photodetectors under chopped visible light illumination (> 400 nm, 35 mW/cm^2) at zero bias. (b), (c) Enlarged rising and recovering edges of J–t curve for 2.0-K sample.

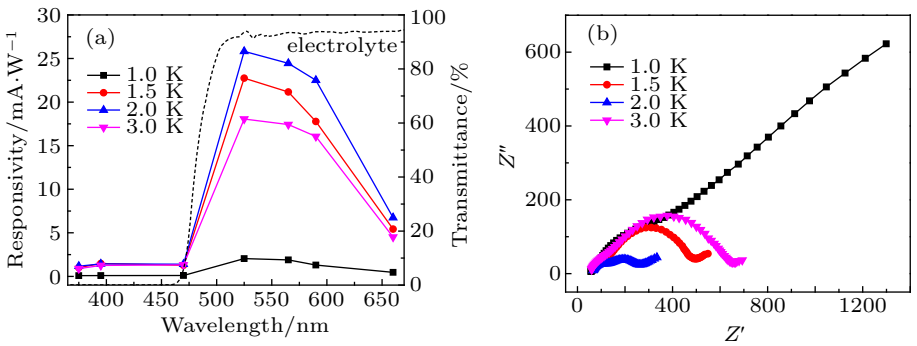


Fig. 5. (a) Plots of photoresponsivity *versus* wavelength of the photodetectors at zero bias, where dash line rtepresents transmittance spectrum of the electrolyte, and (b) EIS plots, for 1.0-K, 1.5-K, 2.0-K, and 3.0-K samples under visible light illumination.

Table 1. Comparison between key parameters of 2.0-K sample and reported parameters of self-powered photodetectors based on Cu_2O nanomaterials.

Materials	Device type	Illumination/nm	Responsivity/(mA/W)	Rising time/ms	Recovering time/ms	Reference
ZnO/Cu_2O	p–n	visible	0.008	90	90	[33]
ZnO/Cu_2O	p–n	UV and visible	0.8	220	320	[34]
ZnO/Cu_2O	PEC	500	2	140	360	[29]
Cu_2O	PEC	525	25.8	5.2	9.0	this work

and 3.0-K samples, respectively. Compared with the reported self-powered photodetectors based on Cu_2O nanomaterials, the 2.0-K sample has an enhanced photoresponsivity and a short response time as shown in Table 1.[29,41,42] To further explore the reason for the optimized performance of the 2.0-K sample, EIS plots of the corresponding photocathodes are demonstrated in Fig. 5(b)). Compared with other samples, the 2.0-K sample has the smallest radius of semicircle of the Nyquist plot, suggesting faster charge transfer at the Cu_2O/electrolyte interface. The Cu_2O particles of the 2.0-K sample are larger in size and have better crystallinity, which increases the concentration of photogenerated carriers and reduces the charger transfer resistance.

4. Conclusions

In this work, the effect of the growth time on the morphology and structure of the Cu_2O films and the photodetection properties of the self-powered photodetectors based on the Cu_2O/electrolyte heterojunctions are studied. As the growth time increases, the size of Cu_2O particles becomes larger, and the 2.0-K film exhibits the highest XRD diffraction peaks. The photodetector based on the 2.0-K film demonstrates a rapid response time (a rising time of 5.2 ms and a recovering time of 9.0 ms) and the highest photoresponsivity of 25.8 mA/W under the 525-nm visible light at zero bias. However, very weak responsivity to UV light is observed due to the strong UV absorption of the electrolyte. The high crystallinity and low charge transfer resistance contribute to the optimized performance of the self-powered photodetector based on the 2.0-K film.

References

[1] Zhang S and Cicoira F 2018 *Nature* **561** 466
[2] Ferreira G, Goswami S, Nandy S, Pereira L, Martins R and Fortunato E 2020 *Adv. Funct. Mater.* **30** 1908994
[3] Wang Z L 2012 *Adv. Mater.* **24** 280
[4] Peng W, Wang X, Yu R, Dai Y, Zou H, Wang A C, He Y and Wang Z L 2017 *Adv. Mater.* **29** 1606698
[5] Ren X, Li Z, Huang Z, Sang D, Qiao H, Qi X, Li J, Zhong J and Zhang H 2017 *Adv. Funct. Mater.* **27** 1606834
[6] Hu L, Yan J, Liao M, Xiang H, Gong X, Zhang L and Fang X 2012 *Adv. Mater.* **24** 2305
[7] Wang C, Xu J, Shi S, Zhang Y, Gao Y, Liu Z, Zhang X and Li L 2017 *J. Phys. Chem. Solids* **103** 218
[8] Hassan J J, Mahdi M A, Kasim S J, Ahmed N M, Abu Hassan H and Hassan Z 2012 *Appl. Phys. Lett.* **101** 261108
[9] Sarkar S and Basak D 2015 *ACS Appl. Mater. Inter.* **7** 16322
[10] Yang S, Gong J and Deng Y 2012 *J. Mater. Chem.* **22** 13899
[11] Hong Q, Cao Y, Xu J, Lu H, He J and Sun J L 2014 *ACS Appl. Mater. Inter.* **6** 20887
[12] Jin W, Ye Y, Gan L, Yu B, Wu P, Dai Y, Meng H, Guo X and Dai L 2012 *J. Mater. Chem.* **22** 2863
[13] Duan L, He F, Tian Y, Sun B, Fan J, Yu X, Ni L, Zhang Y, Chen Y and Zhang W 2017 *ACS Appl. Mater. Inter.* **9** 8161
[14] Wu Y, Yan X, Zhang X and Ren X 2016 *Appl. Phys. Lett.* **109** 183101
[15] Ren X, Li Z, Huang Z, Sang D, Qiao H, Qi X, Li J, Zhong J and Zhang H 2017 *Adv. Funct. Mater.* **27** 1606834
[16] Xie Y, Wei L, Li Q, Chen Y, Yan S, Jiao J, Liu G and Mei L 2014 *Nanotechnology* **25** 075202
[17] Gao C, Li X, Wang Y, Chen L, Pan X, Zhang Z and Xie E 2013 *J. Power Sources* **239** 458
[18] Xie Y R, Wei L, Wei G D, Li Q H, Wang D, Chen Y X, Yan S S, Liu G L, Mei L M and Jiao J 2013 *Nanoscale Res. Lett.* **8** 188
[19] Lee W J and Hon M H 2011 *Appl. Phys. Lett.* **99** 251102
[20] Lin P, Yan X, Liu Y, Li P, Lu S and Zhang Y 2014 *Phys. Chem. Chem. Phys.* **16** 26697
[21] Chen L, Li X, Wang Y, Gao C, Zhang H, Zhao B, Teng F, Zhou J, Zhang Z, Pan X and Xie E 2014 *J. Power Sources* **272** 886
[22] Xie Y, Wei L, Li Q, Chen Y, Liu H, Yan S, Jiao J, Liu G and Mei L 2014 *Nanoscale* **6** 9116
[23] Li X, Gao C, Duan H, Lu B, Wang Y, Chen L, Zhang Z, Pan X and Xie E 2013 *Small* **9** 2005
[24] Gao C, Li X, Zhu X, Chen L, Wang Y, Teng F, Zhang Z, Duan H and Xie E 2014 *J. Alloys Compd.* **616** 510
[25] Susman M D, Feldman Y, Vaskevich A and Rubinstein I 2014 *ACS Nano* **8** 162
[26] Chen X, Lin P, Yan X, Bai Z, Yuan H, Shen Y, Liu Y, Zhang G, Zhang Z and Zhang Y 2015 *ACS Appl. Mater. Inter.* **7** 3216
[27] Paracchino A, Laporte V, Sivula K, Gratzel M and Thimsen E 2011 *Nat. Mater.* **10** 456
[28] Hossain M A, Al-Gaashani R, Hamoudi H, Al Marri M J, Hussein I A, Belaidi A, Merzougui B A, Alharbi F H and Tabet N 2017 *Mater. Sci. Semicon. Proc.* **63** 203
[29] Bai Z and Zhang Y 2016 *J. Alloys Compd.* **675** 325
[30] Bai Z, Liu J, Liu F and Zhang Y 2017 *J. Alloys Compd.* **726** 803
[31] Herbadji A, Bouderbala I Y, Mentar L and Azizi A 2019 *Russ. J. Electrochem.* **55** 1336
[32] Laidoudi S, Bioud A Y, Azizi A, Schmerber G, Bartringer J, Barre S and Dinia A 2013 *Semicond. Sci. Technol.* **28** 115005
[33] Bai Z and Zhang Y 2017 *J. Alloys Compd.* **698** 133
[34] Paracchino A, Brauer J C, Moser J E, Thimsen E and Graetzel M 2012 *J. Phys. Chem. C* **116** 7341
[35] Zou X, Fan H, Tian Y and Yan S 2014 *CrystEngComm* **16** 1149
[36] Matthew S and Kyoung-shin J C 2004 *Adv. Mater.* **16** 1743
[37] Zhai Y C, Fan H Q, Li Q and Yan W 2012 *Appl. Surf. Sci.* **258** 3232
[38] Brandt I S, Martins C A, ZoldanV C, Viegas A D C, Silva J H and Pasa A A 2014 *Thin Solid Films* **562** 144
[39] Brandt I S, Tumelero M A, Pelegrini S, Zangari G and Pasa A A 2017 *J. Solid State Electrochem.* **21** 1999
[40] Zhong Z, Li M, Fu J H, Wang Y X, Muhammad Y, Li S H, Wang J H, Zhao Z X and Zhao Z X 2020 *Chem. Eng. J.* **395** 125184
[41] Ghamgosar P, Rigoni F, You S, Dobryden I, Kohan M G, Pellegrino A L, Concina I, Almqvist N, Malandrino G and Vomiero A 2018 *Nano Energy* **51** 308
[42] Lin P, Chen X, Yan X, Zhang Z, Yuan H, Li P, Zhao Y and Zhang Y 2014 *Nano Research* **7** 860